Available online at www.sciencedirect.com
SCIENCE DIRECT®
Computer Aided Geometric Design 23 (2006) 193–207
COMPUTER AIDED GEOMETRIC DESIGN
www.elsevier.com/locate/cagd

Convergence analysis of a discretization scheme for Gaussian curvature over triangular surfaces

Guoliang Xu [1]

LSEC, Institute of Computational Mathematics, Academy of Mathematics and System Sciences, Chinese Academy of Sciences, Beijing, China

Received 9 March 2005; received in revised form 7 July 2005; accepted 8 July 2005

Available online 10 August 2005

Abstract

In this paper, we study the convergence property of a well known discretized scheme for approximating Gaussian curvature, derived from Gauss–Bonnet theorem, over triangulated surface. Suppose the triangulation is obtained from a sampling of a smooth parametric surface, we show theoretically that the approximation has quadratic convergence rate if the surface sampling satisfies the so-called parallelogram criterion. Numerical results which justify the theoretical analysis are also presented.

Keywords: Gaussian curvature; Surface triangulation; Convergence; Parallelogram criterion

1. Introduction

Gaussian curvature is one of the most essential geometric invariants for surfaces, and it has been extensively used in many fields such as image processing, surface processing, computer aided geometric design and computer graphics. However, this invariant is well defined only for analytically represented and C^2 smooth surfaces. In practice, surface datum are often available as polygonal meshes, typically

E-mail address: xuguo@lsec.cc.ac.cn (G. Xu).

[1] Partially supported by Natural Science Foundation of China (10371130) and National Key Basic Research Project of China (2004CB318000).

0167-8396/$ – see front matter
doi:10.1016/j.cagd.2005.07.002

surface triangulation. Therefore, there is a tremendous need for curvature estimation or approximation from discrete surface meshes.

In the past decades, many discretized approaches for Gaussian curvature have been proposed and used. One class of these approaches is based on the local fitting techniques, such as paraboloid fitting (see (Hamann, 1993; Krsek et al., 1997; Stokely and Wu, 1992)), quadratic fitting (see (Meek and Walton, 2000; Xu, 2004b)) or higher order fitting (see (Cazals and Pouget, 2005)), circular fitting (see (Chen and Schmitt, 1992; Martin, 1998)) and implicit fitting by 3D a function (see (Douros and Buxton, 2002)). In these approaches, a fitting function which approximates the surface data locally is constructed, then the curvature is computed analytically from the fitting function. The second class of methods is based on a theorem for the Gauss map (see (Meek and Walton, 2000; Peng et al., 2003)). For a given neighborhood of a surface point, the theorem says that the Gaussian curvature at the surface point can be approximated by the ratio of the area of the spherical image of the neighborhood and the area of the neighborhood itself. The third class of approaches is based on the Gauss–Bonnet theorem (see (Alboul and van Damme, 1995; Dyn et al., 2001; Kim et al., 2002; Meek and Walton, 2000; Stokely and Wu, 1992)). Assuming the Gaussian curvature is approximately a constant in a surface region with a piecewise smooth curve boundary, a discrete approximation of the Gaussian curvature is obtained by the Gauss–Bonnet theorem (see the next section for details). The derived scheme for triangulated surfaces is usually called *angle deficit scheme* or *Gauss–Bonnet scheme*. Apart from these classes, there are some other approaches, e.g., Taubin's approach (Taubin, 1995) based on the eigen-analysis, Watanabe and Belyaev's approach (see (Watanabe and Belyaev, 2001)) based on the integral formulas of the normal curvature and its square, Wollmann's approach (see (Wollmann, 2000)) based on Euler theorem (see (Do Carmo, 1976, p. 145)) and Meusnier theorem (see (Do Carmo, 1976, p. 142)). Using the theory of normal cycles, Cohen-Steiner and Morvan derive an efficient and reliable curvature estimation algorithm (see (Cohen-Steiner and Morvan, 2003)). Error bound of the estimated curvature is given in the case restricted Delaunay triangulations. In (2003), Surazhsky et al. compare five approaches of the discretization by numerical experiments. The conclusion they draw is that *the best algorithm for the estimation of total* (*Gaussian*) *curvature is the Gauss–Bonnet scheme*.

In this paper, we analyze the convergence of the Gauss–Bonnet scheme, which has been shown the best among the five approaches in (Surazhsky et al., 2003). The convergence of this discretized scheme has been considered by Meek and Walton (2000), the result they obtained is (see Lemmas 4.4 and 5.4 of (Meek and Walton, 2000)): *For non-uniform or uniform data, the angle deficit method approximates the curvature to accuracy* $O(1)$. The approximation accuracy $O(1)$ means that the scheme does not converge. Hence, in Meek and Walton (2000) paper, the authors make a comment as follows: *One surprising result is that the angle deficit method, which is a very popular method in the literature, is not necessarily very accurate*. However, we will prove in this paper that if the surface triangulation is obtained from sampling a parametric surface, then under certain conditions (parallelogram criterion), the approximation accuracy can be $O(h^2)$, meaning the approximation converges with a quadratic rate. This result justifies Surazhsky et al.'s conclusion drawn from the numerical experiments.

An elegant asymptotic estimation for the angular deficit has been given by Borrelli et al. (2003) under regular assumptions. Let $\mathbf{p}$ be a vertex of a triangular mesh with valence n and let $\mathbf{p}_j s$ be the one ring neighbors of $\mathbf{p}$. Borrelli et al. show that if the mesh around the vertex $\mathbf{p}$ is regular, then the angular deficit is asymptotically equivalent to a homogeneous polynomial of degree two in the principal curvatures with closed forms coefficients. Furthermore, if n is six, then the Gauss–Bonnet scheme converges to the exact

Gaussian curvature in the linear rate $O(h)$. By regular mesh, they refer a mesh such that the $\mathbf{p}_j s$ lie in normal sections two consecutive of which form an angle of $2\pi/n$, with the additional constraint that $\|\mathbf{p} - \mathbf{p}_j\|$ is a constant. We will explain later that this result is a special case of ours. Also this result is weaker than ours in the sense that our convergence is in the quadratic rate $O(h^2)$.

The rest of the paper is organized as follows. In Section 2, we describe in detail the discretizations of Gaussian curvature from local Gauss–Bonnet theorem, following Surazhsky et al., we refer to this discretization as *Gauss–Bonnet scheme*. In Section 3, we show numerically the convergence/un-convergence property of the Gauss–Bonnet scheme, and then in Section 4, we give and prove a few theoretical convergence results. The relationship between our results and Borrelli et al.'s is also discussed in this section. Section 5 concludes the paper.

2. Gaussian curvature and its discretization

Let $\mathbf{F}(\xi_1, \xi_2) \in \mathbb{R}^3$ be a regular C^2 parametric surface, let $\mathbf{p} = \mathbf{F}(\xi_1, \xi_2)$ be a surface point and

$$\mathbf{t}_i = \frac{\partial F(\xi_1, \xi_2)}{\partial \xi_i}, \quad \mathbf{t}_{ij} = \frac{\partial^2 F(\xi_1, \xi_2)}{\partial \xi_i \partial \xi_j}, \quad i, j = 1, 2.$$

Then from differential geometry (see (Do Carmo, 1976)), the Gaussian curvature is given by

$$K(\mathbf{p}) = \frac{LN - M^2}{g_{11}g_{22} - g_{12}^2},$$

where

$$g_{11} = \langle \mathbf{t}_1, \mathbf{t}_1 \rangle = \mathbf{t}_1^{\mathrm{T}}\mathbf{t}_1, \quad g_{12} = \langle \mathbf{t}_1, \mathbf{t}_2 \rangle = \mathbf{t}_1^{\mathrm{T}}\mathbf{t}_2, \quad g_{22} = \langle \mathbf{t}_2, \mathbf{t}_2 \rangle = \mathbf{t}_2^{\mathrm{T}}\mathbf{t}_2,$$
$$L = \langle \mathbf{n}, \mathbf{t}_{11} \rangle = \mathbf{n}^{\mathrm{T}}\mathbf{t}_{11}, \quad M = \langle \mathbf{n}, \mathbf{t}_{12} \rangle = \mathbf{n}^{\mathrm{T}}\mathbf{t}_{12}, \quad N = \langle \mathbf{n}, \mathbf{t}_{22} \rangle = \mathbf{n}^{\mathrm{T}}\mathbf{t}_{22},$$

and $\mathbf{n} = \frac{\mathbf{t}_1 \times \mathbf{t}_2}{\|\mathbf{t}_1 \times \mathbf{t}_2\|}$ is the unit normal. In the proof of our convergence result, we will use another expression from (Xu and Bajaj, 2003)

$$K(\mathbf{p}) = \frac{\mathbf{t}_{11}^{\mathrm{T}} Q \mathbf{t}_{22} - \mathbf{t}_{12}^{\mathrm{T}} Q \mathbf{t}_{12}}{\det(G)}, \tag{2.1}$$

where

$$Q = I - [\mathbf{t}_1, \mathbf{t}_2] G^{-1} [\mathbf{t}_1, \mathbf{t}_2]^{\mathrm{T}} \in \mathbb{R}^{3\times 3}, \qquad G = \begin{bmatrix} g_{11} & g_{12} \\ g_{21} & g_{22} \end{bmatrix}.$$

Let D be a region of surface $\mathbf{F}$, whose boundary consists of piecewise smooth curves $\Gamma_j s$. Then the local Gauss–Bonnet theorem (see (Do Carmo, 1976, p. 268)) is as follows

$$\iint_D K(\mathbf{p})\, \mathrm{d}A + \sum \int_{\Gamma_j} k_g(\Gamma_j)\, \mathrm{d}s + \sum \alpha_j = 2\pi,$$

where $k_g(\Gamma_j)$ is the geodesic curvature of the boundary curve Γ_j, α_j is the exterior angle at the jth corner point $\mathbf{p}_j$ of the boundary (see the left figure of Fig. 1). Hence if all the $\Gamma_j s$ are the geodesic curves, the above formula reduces to

$$\iint_D K(\mathbf{p})\, \mathrm{d}A = 2\pi - \sum \alpha_j. \tag{2.2}$$

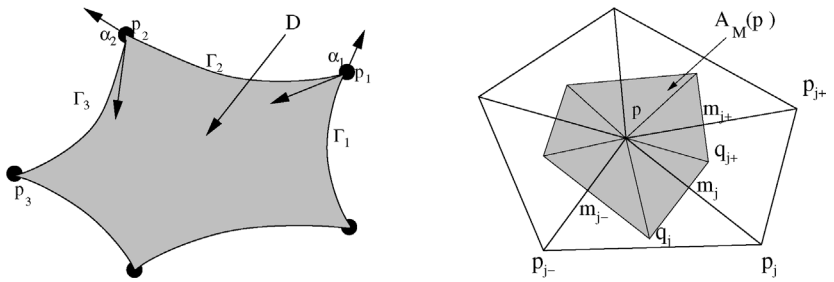

Fig. 1. Left: A region D on surface $\mathbf{F}$ with boundary curves Γ_j and exterior angle α_j at corner $\mathbf{p}_j$. Right: The definition of the area $A_M(\mathbf{p})$.

Now we consider the discretization of $K(\mathbf{p})$. Let M be a triangulation of surface $\mathbf{F}$. For vertex $\mathbf{p}$ of valence n, denote by $\{\mathbf{p}_j\}_{j=1}^n$ the set of the one-ring neighbor vertices of $\mathbf{p}$. We assume in the following that these $\mathbf{p}_1, \ldots, \mathbf{p}_n$ are arranged such that the triangles $[\mathbf{p}\mathbf{p}_j\mathbf{p}_{j-1}]$ and $[\mathbf{p}\mathbf{p}_j\mathbf{p}_{j+1}]$ are in M, and $\mathbf{p}_{j-1}$, $\mathbf{p}_{j+1}$ opposite to the edge $[\mathbf{p}\mathbf{p}_j]$. For $j = 1, \ldots, n$, we use j_+ and j_- to denote $j+1$ and $j-1$, respectively, for simplifying the notation. Furthermore, we use the following conventions throughout the paper: $\mathbf{p}_{n+1} = \mathbf{p}_1$ and $\mathbf{p}_0 = \mathbf{p}_n$.

Assuming $K(\mathbf{p})$ is a constant in the neighborhood of $\mathbf{p}$, and using Eq. (2.2) on the shaded region of Fig. 1 (right), we obtain

$$K^{(1)}(\mathbf{p}) = \frac{3(2\pi - \sum \theta_j)}{A(\mathbf{p})}, \tag{2.3}$$

$$K^{(2)}(\mathbf{p}) = \frac{2\pi - \sum \theta_j}{A_M(\mathbf{p})}, \tag{2.4}$$

where $A(\mathbf{p})$ is the sum of areas of triangles $[\mathbf{p}\mathbf{p}_j\mathbf{p}_{j_+}]$, $A_M(\mathbf{p})$ is the area of the region as shown in the right figure of Fig. 1, θ_j is the angle $\angle \mathbf{p}_j\mathbf{p}\mathbf{p}_{j_+}$. Formula (2.4) has been given by Meyer et al. (2002) based on the Voronoi diagram. Since $A(\mathbf{p})$ could be approximated by $3A_M(\mathbf{p})$ under some conditions (see the condition of Theorem 4.1), (2.3) is easily derived from (2.4).

3. Numerical experiments

The aim of this section is to exhibit the numerical behaviors of the Gauss–Bonnet scheme defined by (2.3)–(2.4), and determine when it converges numerically to the exact value. To show the numerical convergence, we take several two variable functions $f_\beta(x, y)$, from (Franke, 1982), over xy-plane as surfaces in $\mathbb{R}^3$ so that the exact Gaussian curvatures can be easily computed. Both the exact and approximated Gaussian curvatures are computed at some selected domain points $(x_i, y_j) \in [0, 1] \times [0, 1]$. These points are chosen as $(x_i, y_j) = (\frac{i}{20}, \frac{j}{20})$ for $i = 1, \ldots, 19$, $j = 1, \ldots, 19$. The surfaces are triangulated around (x_i, y_j) by triangulating the domain first, and then mapping the planar triangulation onto the surfaces by the selected bivariate functions. The domain around (x_i, y_j) is triangulated locally by choosing n regularly distributed points:

$$\mathbf{q}_k = (x_i, y_j) + r(\cos\theta_k,\ \sin\theta_k),\ \theta_k = 2(k-1)\pi/n, \quad k = 1, \ldots, n. \tag{3.1}$$

The convergence property and the convergence rate are checked by taking $r = 1/8, 1/16, 1/32, \ldots$. The vertex valence n are taken to be $3, 4, \ldots, 9$. The functions we use are the following

$$\begin{aligned}
f_1(x,y) &= 0.75\exp\{-[(9x-2)^2+(9y-2)^2]/4\}\\
&\quad + 0.75\exp\{-[(9x+1)^2/49+(9y+1)/10]\}\\
&\quad + 0.5\exp\{-[(9x-7)^2+(9y-3)^2]/4\}\\
&\quad - 0.2\exp\{-[(9x-4)^2+(9y-7)^2]\},\\
f_2(x,y) &= [\tanh(9y-9x)+1]/9,\\
f_3(x,y) &= \frac{1.25+\cos(5.4y)}{6+6(3x-1)^2},\\
f_4(x,y) &= \exp\{-(81/16)[(x-0.5)^2+(y-0.5)^2]\}/3,\\
f_5(x,y) &= \sqrt{(8/9)^2-(x-0.5)^2-(y-0.5)^2}-0.5.
\end{aligned}$$

Here we regard the graphs of the functions $f_\beta(x,y)$ as parametric surfaces

$$\mathbf{F}_\beta(x,y) = [x, y, f_\beta(x,y)]^{\mathrm{T}} \in \mathbb{R}^3, \quad \beta = 1, \ldots, 5.$$

The numerical experiments show that as $r \to 0$, the maximal errors of the approximated Gaussian curvature computed by $K^{(\alpha)}$ over the above mentioned local triangulations and the exact Gaussian curvature computed from the continuous surfaces defined by f_β tend asymptotically to the form $e_\alpha(f_\beta, n) := C_{\alpha\beta}^{(k)} r^k$ for a constant $C_{\alpha\beta}^{(k)}$ and an integer k. Tables 1 and 2 show the asymptotic maximal error $e_1(f_\beta, n)$ and $e_2(f_\beta, n)$, respectively.

Table 1
The asymptotic maximal errors $e_1(f_\beta, n)$, $\beta = 1, \ldots, 5$

n	$e_1(f_1,n)$	$e_1(f_2,n)$	$e_1(f_3,n)$	$e_1(f_4,n)$	$e_1(f_5,n)$
3	1.7451e+03	5.4848e+01	5.4591e+01	2.1477e+01	3.5665e+00
4	4.3638e+02	2.7425e+01	1.3088e+01	5.3697e+00	1.1504e+00
5	1.2730e+02	4.0015e+00	3.9825e+00	1.5667e+00	2.6017e−01
6	$3.0326e{+}05 * r^2$	$3.2709e{+}02 * r^2$	$4.6461e{+}02 * r^2$	$9.3499e{+}01 * r^2$	$1.7389e{+}00 * r^2$
7	6.6370e+01	2.0857e+00	2.0763e+00	8.1683e−01	1.3564e−01
8	1.0586e+02	3.3271e+00	3.3116e+00	1.3028e+00	2.1634e−01
9	1.3144e+02	4.1309e+00	4.1120e+00	1.6177e+00	2.6863e−01

Table 2
The asymptotic maximal errors $e_2(f_\beta, n)$, $\beta = 1, \ldots, 5$

n	$e_1(f_1,n)$	$e_1(f_2,n)$	$e_1(f_3,n)$	$e_1(f_4,n)$	$e_1(f_5,n)$
3	8.7292e+02	3.6566e+01	2.7675e+01	1.0739e+01	1.9558e+00
4	4.6945e+01	1.9725e+01	1.3138e+00	9.5933e−01	6.4778e−01
5	2.5406e+01	3.4720e+00	1.4877e+00	1.8575e−01	6.0622e−02
6	$2.3771e{+}05 * r^2$	$3.7523e{+}02 * r^2$	$4.0240e{+}02 * r^2$	$8.3667e{+}01 * r^2$	$5.8738e{-}01 * r^2$
7	1.6453e+01	2.2659e+00	9.6194e−01	1.2050e−01	4.9649e−03
8	2.7606e+01	3.8101e+00	1.6133e+00	2.0227e−01	2.1116e−02
9	3.5472e+01	4.9030e+00	2.0724e+00	2.5999e−01	4.1987e−02

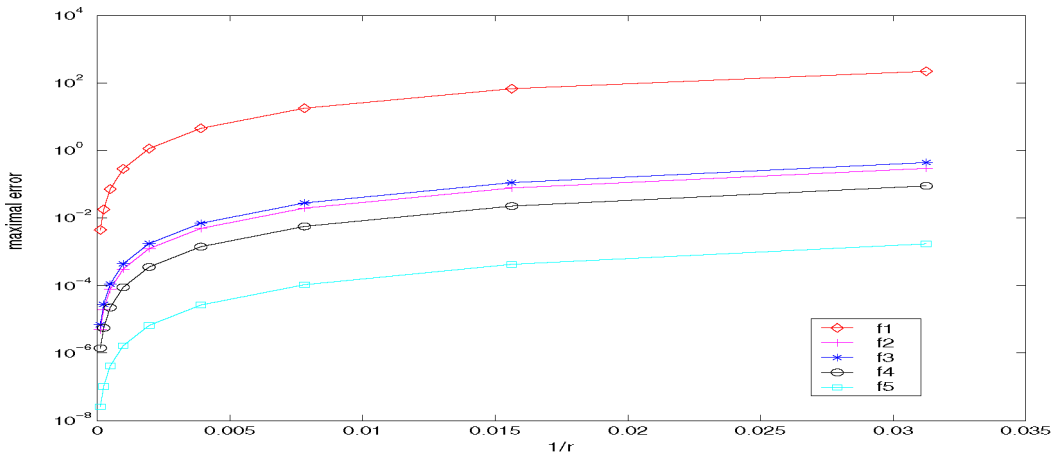

Fig. 2. Maximal errors of $K^{(1)}(\mathbf{p})$ for functions $f_1, \ldots, f_5$ and for $n = 6$. The quadratic convergence rate is clearly observed.

From these numerical results, we can draw the following conclusions for the regularly distributed domain vertices.

1. If the valence n is 6, the approximate curvature converges in the rate $O(r^2)$. Fig. 2 plots the maximal errors of $K^{(1)}(\mathbf{p})$ for functions $f_1, \ldots, f_5$. If $n \neq 6$, the approximation accuracy is $O(1)$. The latter conclusion is consistent with Meek and Walton's results (see (Meek and Walton, 2000)).
2. For a fixed β, the error $e_\alpha(f_\beta, n)$ decreases from $n = 3$ to 6, and then increases from $n = 6$ to 9. That is, the results for $n = 6$ are the best. This is consistent with Surazhsky et al.'s results (see (Surazhsky et al., 2003)).
3. $e_2(f_\beta, n) < e_1(f_\beta, n)$ holds for most of the cases. The exceptional 4 cases, among the 35 cases, are $\beta = 2$, $n = 6, 7, 8, 9$. Hence, $K^{(2)}(\mathbf{p})$ is better than $K^{(1)}(\mathbf{p})$ in general.

Remark 3.1. Though the example surfaces used in this section are graphs of bivariate functions. Our attention in this paper is focused on the general parametric surfaces (see Section 4) which contain functional surfaces as special cases.

4. Convergence of discrete Gaussian curvature

In the previous section, we have shown numerically that the discrete Gaussian curvatures defined by (2.3) and (2.4) converge in some special cases. In this section, we give a sufficient condition for the convergence.

Theorem 4.1. *Let* $\mathbf{p}$ *be a vertex of* M *with valence six, and let* $\mathbf{p}_j$, $j = 1, \ldots, 6$, *be its neighbor vertices. Suppose* $\mathbf{p}$ *and* $\mathbf{p}_j$ $(j = 1, \ldots, 6)$ *are on a sufficiently smooth parametric surface* $\mathbf{F}(\xi_1, \xi_2) \in \mathbb{R}^3$, *and there exist* $\mathbf{q}$, $\mathbf{q}_j \in \mathbb{R}^2$ *such that* (*see Fig.* 3)

$$\mathbf{p} = \mathbf{F}(\mathbf{q}), \quad \mathbf{p}_j = \mathbf{F}(\mathbf{q}_j) \quad \textit{and} \quad \mathbf{q}_j = \mathbf{q}_{j_-} + \mathbf{q}_{j_+} - \mathbf{q}, \quad j = 1, \ldots, 6. \tag{4.1}$$

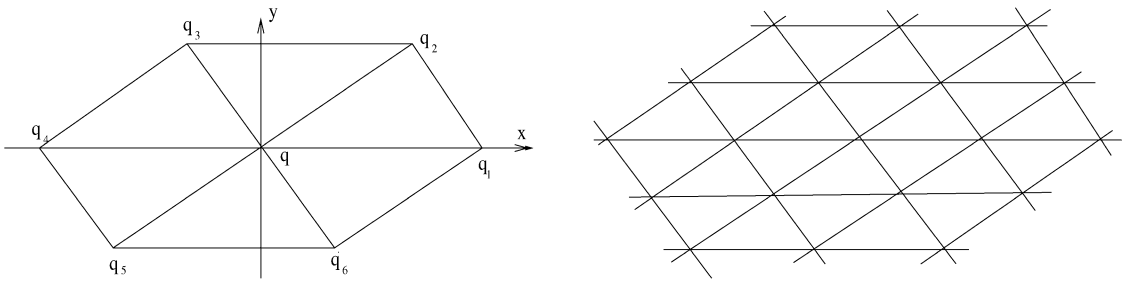

Fig. 3. The triangulations of the domain.

Then

$$\frac{3}{A(\mathbf{p},r)}\left[2\pi-\sum_{j=1}^{6}\theta_j(r)\right]=K(\mathbf{p})+\mathrm{O}(r^2),\quad \text{as } r\to 0, \tag{4.2}$$

where $A(\mathbf{p},r)$ *is the sum of the areas of triangles* $[\mathbf{p}\mathbf{p}_j(r)\mathbf{p}_{j_+}(r)]$ *and*

$$\mathbf{p}_j(r)=\mathbf{F}\big(\mathbf{q}_j(r)\big),\quad \mathbf{q}_j(r)=\mathbf{q}+r(\mathbf{q}_j-\mathbf{q}),\quad j=1,\dots,6. \tag{4.3}$$

Condition (4.1) implies that each of the quadrilaterals $[\mathbf{q}\mathbf{q}_{j_-}\mathbf{q}_j\mathbf{q}_{j_+}]$, $j=1,\dots,6$, is a parallelogram (see Fig. 3). Hence, we refer this condition as *parallelogram criterion*.

Proof of Theorem 4.1. The proof of the theorem is rather complicated. Some derivation is carried out by virtue of Maple. First note that, since

$$\sin\Big(2\pi-\sum\theta_j\Big)=-\sin\sum\theta_j\quad\text{and}\quad \sin x=x+\mathrm{O}(x^3),\quad x\to 0,$$

we only need to prove the following

$$-\frac{3\sin\sum\theta_j(r)}{A(\mathbf{p},r)}=K(\mathbf{p})+\mathrm{O}(r^2). \tag{4.4}$$

Let

$$-3\sin\sum\theta_j(r)=n_0+n_1r+n_2r^2+n_3r^3+\mathrm{O}(r^4), \tag{4.5}$$

$$A(\mathbf{p},r)=a_0r^2+a_1r^3+\mathrm{O}(r^4), \tag{4.6}$$

be the Taylor expansions in r of the numerator and denominator of the left-handed side of (4.4), respectively. We will prove

$$n_0=0,\quad n_1=0,\quad n_3=0,\quad a_1=0, \tag{4.7}$$

and

$$n_2/a_0=K(\mathbf{p}). \tag{4.8}$$

These relations imply (4.4).

Without loss of generality, we may assume $\mathbf{q}=[0,0]^{\mathrm{T}}$, $\mathbf{q}_1=[1,0]^{\mathrm{T}}$. Then there exists a constant $a>0$ and an angle θ such that

$$\mathbf{q}_2=[a\cos\theta,a\sin\theta]^{\mathrm{T}}.$$

Hence, $\mathbf{q}_3 = [a\cos\theta - 1, a\sin\theta]^{\mathrm{T}}$, $\mathbf{q}_{j+3} = -\mathbf{q}_j$, $j = 1, 2, 3$. Let

$$\mathbf{q}_j = s_j\mathbf{d}_j = s_j[g_j, l_j]^{\mathrm{T}}, \quad j = 1, \ldots, 6,$$

where $s_j = \|\mathbf{q}_j\|$, $\|\mathbf{d}_j\| = 1$. Then

$$\begin{aligned}
&s_1 = 1, \quad s_2 = a, \quad s_3 = \sqrt{a^2 - 2ac + 1}, \quad s_4 = s_1, \quad s_5 = s_2, \quad s_6 = s_3,\\
&g_1 = 1, \quad g_2 = c, \quad g_3 = (ac - 1)/s_3, \quad g_4 = -g_1, \quad g_5 = -g_2, \quad g_6 = -g_3,\\
&l_1 = 0, \quad l_2 = t, \quad l_3 = at/s_3, \quad l_4 = -l_1, \quad l_5 = -l_2, \quad l_6 = -l_3,
\end{aligned}$$

where $(c, t) := (\cos\theta, \sin\theta)$. Let $\mathbf{F}^k_{\mathbf{d}_j}$ denote the kth order directional derivative of $\mathbf{F}$ in the direction $\mathbf{d}_j$. Then using Taylor expansion in r, we have

$$\mathbf{p}_j(r) - \mathbf{p} = s_j r\mathbf{F}_{\mathbf{d}_j} + \frac{1}{2}s_j^2 r^2\mathbf{F}^2_{\mathbf{d}_j} + \frac{1}{6}s_j^3 r^3\mathbf{F}^3_{\mathbf{d}_j} + \frac{1}{24}s_j^4 r^4\mathbf{F}^4_{\mathbf{d}_j} + \mathrm{O}(r^5), \tag{4.9}$$

$$\begin{aligned}
\big\|\mathbf{p}_j(r) - \mathbf{p}\big\|^2 = {}& s_j^2 r^2\langle\mathbf{F}_{\mathbf{d}_j}, \mathbf{F}_{\mathbf{d}_j}\rangle + s_j^3 r^3\big\langle\mathbf{F}_{\mathbf{d}_j}, \mathbf{F}^2_{\mathbf{d}_j}\big\rangle + \frac{1}{4}s_j^4 r^4\big\langle\mathbf{F}^2_{\mathbf{d}_j}, \mathbf{F}^2_{\mathbf{d}_j}\big\rangle + \frac{1}{3}s_j^4 r^4\big\langle\mathbf{F}_{\mathbf{d}_j}, \mathbf{F}^3_{\mathbf{d}_j}\big\rangle\\
&+ \frac{1}{6}s_j^5 r^5\big\langle\mathbf{F}^2_{\mathbf{d}_j}, \mathbf{F}^3_{\mathbf{d}_j}\big\rangle + \frac{1}{12}s_j^5 r^5\big\langle\mathbf{F}_{\mathbf{d}_j}, \mathbf{F}^4_{\mathbf{d}_j}\big\rangle + \mathrm{O}(r^6),
\end{aligned} \tag{4.10}$$

$$\begin{aligned}
\big\langle\mathbf{p}_j(r) - \mathbf{p}, \mathbf{p}_{j_+}(r) - \mathbf{p}\big\rangle = {}& s_j s_{j_+} r^2\langle\mathbf{F}_{\mathbf{d}_j}, \mathbf{F}_{\mathbf{d}_{j_+}}\rangle + \frac{1}{2}s_j s_{j_+}^2 r^3\big\langle\mathbf{F}_{\mathbf{d}_j}, \mathbf{F}^2_{\mathbf{d}_{j_+}}\big\rangle + \frac{1}{2}s_j^2 s_{j_+} r^3\big\langle\mathbf{F}_{\mathbf{d}_{j_+}}, \mathbf{F}^2_{\mathbf{d}_j}\big\rangle\\
&+ \frac{1}{4}s_j^2 s_{j_+}^2 r^4\big\langle\mathbf{F}^2_{\mathbf{d}_j}, \mathbf{F}^2_{\mathbf{d}_{j_+}}\big\rangle + \frac{1}{6}s_j s_{j_+}^3 r^4\big\langle\mathbf{F}_{\mathbf{d}_j}, \mathbf{F}^3_{\mathbf{d}_{j_+}}\big\rangle + \frac{1}{6}s_j^3 s_{j_+} r^4\big\langle\mathbf{F}_{\mathbf{d}_{j_+}}, \mathbf{F}^3_{\mathbf{d}_j}\big\rangle\\
&+ \frac{1}{12}s_j^2 s_{j_+}^3 r^5\big\langle\mathbf{F}^2_{\mathbf{d}_j}, \mathbf{F}^3_{\mathbf{d}_{j_+}}\big\rangle + \frac{1}{12}s_{j_+}^2 s_j^3 r^5\big\langle\mathbf{F}^2_{\mathbf{d}_{j_+}}, \mathbf{F}^3_{\mathbf{d}_j}\big\rangle\\
&+ \frac{1}{24}s_j s_{j_+}^4 r^5\big\langle\mathbf{F}_{\mathbf{d}_j}, \mathbf{F}^4_{\mathbf{d}_{j_+}}\big\rangle + \frac{1}{24}s_{j_+} s_j^4 r^5\big\langle\mathbf{F}_{\mathbf{d}_{j_+}}, \mathbf{F}^4_{\mathbf{d}_j}\big\rangle + \mathrm{O}(r^6).
\end{aligned} \tag{4.11}$$

We will explain later that why the order of the expansions above is required up to 5. Now we need to compute all the inner products in (4.10) and (4.11). Let

$$\mathbf{t}_{ijk} = \frac{\partial^3 F}{\partial\xi_i\partial\xi_j\partial\xi_k}, \quad \mathbf{t}_{ijkl} = \frac{\partial^4 F}{\partial\xi_i\partial\xi_j\partial\xi_k\partial\xi_l}, \quad i, j, k, l = 1, 2.$$

Then we have

$$\mathbf{F}_{\mathbf{d}_j} = g_j\mathbf{t}_1 + l_j\mathbf{t}_2, \tag{4.12}$$

$$\mathbf{F}^2_{\mathbf{d}_j} = g_j^2\mathbf{t}_{11} + 2g_j l_j\mathbf{t}_{12} + l_j^2\mathbf{t}_{22}, \tag{4.13}$$

$$\mathbf{F}^3_{\mathbf{d}_j} = g_j^3\mathbf{t}_{111} + 3g_j^2 l_j\mathbf{t}_{112} + 3g_j l_j^2\mathbf{t}_{122} + l_j^3\mathbf{t}_{222}, \tag{4.14}$$

$$\mathbf{F}^4_{\mathbf{d}_j} = g_j^4\mathbf{t}_{1111} + 4g_j^3 l_j\mathbf{t}_{1112} + 6g_j^2 l_j^2\mathbf{t}_{1122} + 4g_j l_j^3\mathbf{t}_{1222} + l_j^4\mathbf{t}_{2222}. \tag{4.15}$$

Let

$$g_{ijk} = \mathbf{t}_i^{\mathrm{T}}\mathbf{t}_{jk}, \quad g_{ijkl} = \mathbf{t}_{ij}^{\mathrm{T}}\mathbf{t}_{kl}, \quad e_{ijkl} = \mathbf{t}_i^{\mathrm{T}}\mathbf{t}_{jkl}, \quad e_{ijklm} = \mathbf{t}_i^{\mathrm{T}}\mathbf{t}_{jklm}, \quad f_{ijklm} = \mathbf{t}_{ij}^{\mathrm{T}}\mathbf{t}_{klm}.$$

Then from (4.12)–(4.15), it is easy to see that all the inner products in (4.10) and (4.11) can be expressed as linear combinations of g_{ij}, g_{ijk}, g_{ijkl}, e_{ijkl}, e_{ijklm} and f_{ijklm}. For example,

$$\langle \mathbf{F}_{\mathbf{d}_j}, \mathbf{F}_{\mathbf{d}_j} \rangle = g_j^2 g_{11} + 2 g_j l_j g_{12} + l_j^2 g_{22};$$
$$\langle \mathbf{F}_{\mathbf{d}_j}^2, \mathbf{F}_{\mathbf{d}_j}^2 \rangle = g_j^4 g_{1111} + 4 g_j^2 l_j^2 g_{1212} + l_j^4 g_{2222} + 4 g_j^3 l_j g_{1112} + 2 g_j^2 l_j^2 g_{1122} + 4 g_j l_j^3 g_{1222}.$$

All the required inner products are given in Appendix A.

Repeatedly using the formulas $\sin(\alpha+\beta) = \sin\alpha\cos\beta + \cos\alpha\sin\beta$ and $\cos(\alpha+\beta) = \cos\alpha\cos\beta - \sin\alpha\sin\beta$, we can derive that

$$\sin\sum_{j=1}^{6}\theta_j(r) = \sum_{j=1}^{6}\sin\theta_j(r)\prod_{k\neq j}\cos\theta_k(r) + \sum_{j=1}^{6}\cos\theta_j(r)\prod_{k\neq j}\sin\theta_k(r) - \sum_{1\leqslant j_1<j_2<j_3\leqslant 6}\ \prod_{k\in\{j_1,j_2,j_3\}}\cos\theta_k(r)\prod_{k\notin\{j_1,j_2,j_3\}}\sin\theta_k(r), \tag{4.16}$$

where

$$\cos\theta_j(r) = \frac{\langle \mathbf{p}_j(r)-\mathbf{p}, \mathbf{p}_{j_+}(r)-\mathbf{p}\rangle}{\|\mathbf{p}_j(r)-\mathbf{p}\|\|\mathbf{p}_{j_+}(r)-\mathbf{p}\|}, \tag{4.17}$$

$$\sin\theta_j(r) = \frac{\sqrt{\|\mathbf{p}_j(r)-\mathbf{p}\|^2\|\mathbf{p}_{j_+}(r)-\mathbf{p}\|^2 - \langle \mathbf{p}_j(r)-\mathbf{p}, \mathbf{p}_{j_+}(r)-\mathbf{p}\rangle^2}}{\|\mathbf{p}_j(r)-\mathbf{p}\|\|\mathbf{p}_{j_+}(r)-\mathbf{p}\|}. \tag{4.18}$$

Hence all the terms in the right-handed side of (4.16) have the same denominator $\prod_{j=1}^{6}\|\mathbf{p}_j(r)-\mathbf{p}\|^2$. Note that this denominator has a factor r^{12}, since each $\|\mathbf{p}_j(r)-\mathbf{p}\|^2$ has a factor r^2. Similarly, the numerator of each term of the right-handed side of (4.16) also has a factor r^{12}. After the cancellation of this factor, we can see that if we want to expand (4.16) up to order 3, we need to expand $\|\mathbf{p}_j(r)-\mathbf{p}\|^2$ and $\langle \mathbf{p}_j(r)-\mathbf{p}, \mathbf{p}_{j_+}(r)-\mathbf{p}\rangle$ up to order 5. Substituting (4.10) and (4.11) into (4.17) and (4.18), and as well as the following area expression:

$$A(\mathbf{p}, r) = \frac{1}{2}\sum_{j=1}^{6}\sqrt{\left\|\mathbf{p}_j(r)-\mathbf{p}\right\|^2\left\|\mathbf{p}_{j_+}(r)-\mathbf{p}\right\|^2 - \left\langle \mathbf{p}_j(r)-\mathbf{p}, \mathbf{p}_{j_+}(r)-\mathbf{p}\right\rangle^2},$$

and then substituting (4.17) and (4.18) into (4.16), and using Maple (we use Maple version 7) to conduct all the symbolic calculation, we arrive at (4.7) and

$$a_0 = 3\sqrt{a^2t^2(-g_{12}^2 + g_{22}g_{11})}, \tag{4.19}$$

$$\begin{aligned} n_2 = {} & -3\sqrt{a^2t^2(-g_{12}^2 + g_{22}g_{11})}(-g_{22}g_{112}^2 - g_{11}g_{212}^2 - g_{1212}g_{12}^2 + g_{1212}g_{22}g_{11} \\ & + g_{1122}g_{12}^2 - g_{1122}g_{22}g_{11} + g_{22}g_{122}g_{111} - g_{12}g_{122}g_{211} + 2g_{12}g_{212}g_{112} - g_{12}g_{222}g_{111} \\ & + g_{11}g_{211}g_{222})/(-g_{12}^2 + g_{22}g_{11})^2. \end{aligned}$$

Therefore,

$$\begin{aligned} \frac{n_2}{a_0} &= -(g_{1212}g_{22}g_{11} - g_{1212}g_{12}^2 - g_{1122}g_{22}g_{11} + g_{1122}g_{12}^2 - g_{22}g_{112}^2 - g_{11}g_{212}^2 + g_{11}g_{222}g_{211} \\ &\quad + 2g_{12}g_{112}g_{212} - g_{12}g_{111}g_{222} - g_{12}g_{211}g_{122} + g_{22}g_{122}g_{111})/(g_{22}g_{11} - g_{12}^2)^2 \\ &= \left[(g_{1122-}g_{1212})\det(G) + g_{11}(g_{212}^2 - g_{211}g_{222}) + g_{22}(g_{112}^2 - g_{111}g_{122})\right. \\ &\quad \left. + g_{12}(g_{111}g_{222} + g_{211}g_{122} - 2g_{112}g_{212})\right]/\det(G)^2. \end{aligned}$$

It follows from (2.1) that n_2/a_0 is just $K(\mathbf{p})$. This completes the proof of the theorem. □

Remark 4.1. The calculation of the right-handed side of (4.16) involves a huge number of terms. Without the help of Maple, it is almost impossible to finish the derivation by hand. Maple completes all the computation in 1574 seconds on a PC equipped with a 3.0 GHz Intel(R) CPU. The main cost is the computation of n_3 which is the coefficient of r^3 in (4.5). If n_3 is not computed, the total time cost is 65 seconds. The Maple code that conducts all derivation of the theorem is available in http://lsec.cc.ac.cn/~xuguo/xuguo3.html. The interested readers are encouraged to perform the computation.

Multiplying both sides of (4.2) by $A(\mathbf{p}, r)/3$ and noticing (4.6) and (4.19), we obtain the following corollary.

Corollary 4.1. *Under the conditions of Theorem* 4.1*, we have*

$$2\pi - \sum_{j=1}^{6} \theta_j(r) = \|\mathbf{q}_1 - \mathbf{q}\|\|\mathbf{q}_2 - \mathbf{q}\| \sin\theta \sqrt{\det(G)} r^2 K(\mathbf{p}) + \mathrm{O}(r^4), \quad \text{as } r \to 0, \tag{4.20}$$

where $\theta = \angle \mathbf{q}_1\mathbf{q}\mathbf{q}_2$ *is the angle between the vectors* $\mathbf{q}_2 - \mathbf{q}$ *and* $\mathbf{q}_1 - \mathbf{q}$.

Note that $\|\mathbf{q}_1 - \mathbf{q}\|\|\mathbf{q}_2 - \mathbf{q}\| \sin\theta$ is the area of the parallelogram $[\mathbf{q}\mathbf{q}_1\mathbf{q}_2\mathbf{q}_3]$. If we take $\|\mathbf{q}_2 - \mathbf{q}\| = \|\mathbf{q}_1 - \mathbf{q}\|$, $\theta = \pi/3$ and if the parametric surface $\mathbf{F}(\xi_1, \xi_2)$ satisfy $\det(G) = 1$, then

$$2\pi - \sum_{j=1}^{6} \theta_j(r) = \sqrt{3}/2 \|\mathbf{q}_1 - \mathbf{q}\|^2 r^2 K(\mathbf{p}) + \mathrm{O}(r^4), \quad \text{as } r \to 0. \tag{4.21}$$

This result is formally the same as Borrelli et al.'s if we denote $\|\mathbf{q}_1 - \mathbf{q}\| r$ by η (see (Borrelli et al., 2003, Eq. (15))), except for the remainder which is $\mathrm{O}(r^4)$ instead of $\mathrm{o}(r^2)$.

The parallelogram criterion is a rather restrictive condition. In practice, this condition may be satisfied approximately. Hence, one may ask how large a perturbation of $\mathbf{q}_j(r)$ is allowed such that the convergence conclusion still holds for the perturbed data. From the proof of Theorem 4.1, we easily obtain the following corollary.

Corollary 4.2. *Under the conditions of Theorem* 4.1*, if* $\mathbf{q}_j(r)$ *is perturbed as*

$$\mathbf{q}_j(r) = \mathbf{q} + r(\mathbf{q}_j - \mathbf{q}) + \epsilon_j(r), \quad \epsilon_j(r) \in \mathbb{R}^3,$$

such that

$$\big\|\epsilon_j(r)\big\| \leqslant C_j r^{\alpha}, \quad \alpha \geqslant 3, \quad C_j \text{ is a constant}, \tag{4.22}$$

then for the perturbed data we have

$$\frac{3}{A(\mathbf{p}, r)} \left[2\pi - \sum_{j=1}^{6} \theta_j(r) \right] = K(\mathbf{p}) + \mathrm{O}(r^{\min\{\alpha-3,2\}}), \quad \text{as } r \to 0.$$

Hence, to have a convergence result, α must be great than three. However, if the perturbation $\epsilon_j(r)$ is in the radial direction $\mathbf{q}_j - \mathbf{q}$, then condition (4.22) could be weakened. That is, we have the following corollary.

Corollary 4.3. *Under the conditions of Theorem* 4.1*, if* $\mathbf{q}_j(r)$ *is perturbed as*

$$\mathbf{q}_j(r) = \mathbf{q} + \big(r + \varepsilon_j(r)\big)(\mathbf{q}_j - \mathbf{q}_i), \quad \varepsilon_j(r) \in \mathbb{R},$$

such that

$$\big|\epsilon_j(r)\big| \leqslant C_j r^{\alpha}, \quad \alpha \geqslant 2, \quad C_j \text{ is a constant}, \tag{4.23}$$

then for the perturbed data we have

$$\frac{3}{A(\mathbf{p}, r)}\left[2\pi - \sum_{j=1}^{6} \theta_j(r)\right] = K(\mathbf{p}) + \mathrm{O}(r^{\min\{\alpha-2,2\}}), \quad \text{as } r \to 0.$$

This corollary can be proved in the same way as Theorem 4.1 by replacing r with $r + C_j r^{\alpha}$ in (4.9). We omit the details.

Lemma 4.1 (see (Xu, 2004a))*. Under the conditions of Theorem* 4.1*, we have*

$$\frac{A(\mathbf{p}, r)}{A_M(\mathbf{p}, r)} = 3 + \mathrm{O}(r^2), \quad \text{as } r \to 0,$$

where $A_M(\mathbf{p}, r)$ *is defined as in* (2.4) *from vertices* $\mathbf{p}_j(r)$.

Therefore, we have the following

Theorem 4.2. *Under the conditions of Theorem* 4.1*, we have*

$$\frac{1}{A_M(\mathbf{p}, r)}\left[2\pi - \sum_{j=1}^{6} \theta_j(r)\right] = K(\mathbf{p}) + \mathrm{O}(r^2), \quad \text{as } r \to 0.$$

Remark 4.2. Notice that the convergence results are obtained under a particular condition. This particularity is not only in the position the vertices locate, but also in the valence the vertices have. However, this particular case is very useful and important, because triangulated surfaces can be generated by a uniform three-directional partition of the domain. This kind of domain triangulation satisfies the conditions of Theorem 4.1.

Remark 4.3. It is interesting to note that the convergence condition of Gauss–Bonnet scheme is exactly the same as the convergence condition of a discrete Laplace–Beltrami operator (see (Xu, 2004a)) proposed by Meyer et al. (2002).

Discussion. Now let us explain the relationship between the results in this paper and the results in Borrelli et al.'s (2003) paper for the case $n = 6$. As mentioned in the introduction part, Borrelli et al.'s convergence result holds under a regularity condition. Let S be a smooth surface, $\mathbf{p}$ be a surface point, and $\mathbf{p}_j s$ be the one ring neighbor points of $\mathbf{p}$. The regularity condition is that $\mathbf{p}_j s$ lie in normal sections two consecutive of which form an angle of $\pi/3$, with the additional constraint that $\|\mathbf{p} - \mathbf{p}_j\| = \eta$ is a constant.

Take a Cartesian coordinate system (ξ_1, ξ_2) in the tangent plane at $\mathbf{p}$ with $\mathbf{p}$ the origin—for example, take the principal directions at $\mathbf{p}$ to be the coordinate axes. Then surface S can be regarded as a graph of a bivariate function $f(\xi_1, \xi_2)$ in the neighborhood of $\mathbf{p}$. Let $\mathbf{q} = [0, 0]^{\mathrm{T}}$ and $\mathbf{q}'_j \in \mathbb{R}^2$ such that

$$\mathbf{p}_j = \mathbf{p} + \left[\mathbf{q}_j^{\mathrm{T}}, f(\mathbf{q}_j)\right]^{\mathrm{T}}, \quad j = 1, \ldots, 6.$$

Then, by the facts $f(\mathbf{q}) = 0$ and $\nabla f(\mathbf{q}) = 0$, it is easy to derive that

$$\|\mathbf{q}'_j - \mathbf{q}\| = \|\mathbf{p}_j - \mathbf{p}\| + \mathrm{O}(\eta^3).$$

Let $\rho = \frac{1}{6}\sum_{j=1}^{6} \|\mathbf{q}'_j - \mathbf{q}\|$,

$$\mathbf{q}_j = \mathbf{q} + \rho(\mathbf{q}'_j - \mathbf{q})/\|\mathbf{q}'_j - \mathbf{q}\|, \quad j = 1, \ldots, 6.$$

Then $\mathbf{q}_j s$ are regularly distributed points on the tangent plane ($\|\mathbf{q}_j - \mathbf{q}\| = \rho$, $\angle \mathbf{q}_j \mathbf{q} \mathbf{q}_{j_+} = \pi/3$) and

$$\|\mathbf{q}_j - \mathbf{q}'_j\| = \mathrm{O}(\eta^3).$$

Therefore, $\mathbf{q}'_j$ could be regarded as the result of a third order ($\alpha = 3$ in (4.23)) perturbation of $\mathbf{q}_j$ in the radial direction. Now applying Corollary 4.3 for the sampling points $\mathbf{q}'_j s$ on the tangent plane, we arrive at Borrelli et al.'s result:

$$\frac{3}{A(\mathbf{p}, \eta)}\left[2\pi - \sum_{j=1}^{6} \theta_j(\eta)\right] = K(\mathbf{p}) + \mathrm{O}(\eta), \quad \text{as } \eta \to 0.$$

Hence, Borrelli et al.'s result for $n = 6$ can be derived from our results. The discussion above also explains why the convergence rate of the Gauss–Bonnet scheme for Borrelli et al.'s sampling is linear. The regular sampling on surface is in fact a third order perturbation of the "perfect" sampling (satisfying parallelogram criterion) on the parameter domain. This perturbation degrades the convergence rate from quadratic to linear.

Now we illustrate that the parallelogram criterion is more general than the regularity condition. From the Taylor expansion

$$\mathbf{F}(\mathbf{q}_j) = \mathbf{F}(\mathbf{q}) + \nabla \mathbf{F}(\mathbf{q})^{\mathrm{T}}(\mathbf{q}_j - \mathbf{q}) + \mathrm{O}\big(\|(\mathbf{q}_j - \mathbf{q})\|^2\big),$$

and condition (4.1) we know that surface points $\mathbf{p}_j(r) = \mathbf{F}(\mathbf{q}_j(r))$ satisfy the same relation as $\mathbf{q}_j(r)$ within the error $\mathrm{O}(r^2)$:

$$\mathbf{p}_j(r) = \mathbf{p}_{j_-}(r) + \mathbf{p}_{j_+}(r) - \mathbf{p} + \mathrm{O}(r^2). \tag{4.24}$$

In another word, the first order approximations $\mathbf{p} + r\nabla \mathbf{F}(\mathbf{q})^{\mathrm{T}}(\mathbf{q}_j - \mathbf{q})$ of the surface points $\mathbf{p}_j(r)$ satisfy the parallelogram criterion on the tangent plane of the surface at $\mathbf{q}$. Hence the corresponding tangent plane partition is not necessarily uniform and the length $\|\mathbf{p} - \mathbf{p}_j(r)\|$ are not necessarily constant. Furthermore, we notice that a set of points $\{\mathbf{q}_j\}_{j=1}^{6} \subset \mathbb{R}^2$ around $\mathbf{q}$ satisfying parallelogram criterion is uniquely determined by four parameters: the offset angle α which is defined as the angle between $\mathbf{q}_1 - \mathbf{q}$ and the first coordinate axis, the lengths of $\mathbf{q}_1 - \mathbf{q}$ and $\mathbf{q}_2 - \mathbf{q}$, and the angle $\theta = \angle \mathbf{q}_1 \mathbf{q} \mathbf{q}_2$ (see (4.20)). But a set of points $\{\mathbf{q}'_j\}_{j=1}^{6} \subset \mathbb{R}^2$ around $\mathbf{q}$ satisfying regularity condition is uniquely determined by two parameters: the offset angle α and the length of $\mathbf{q}_1 - \mathbf{q}$ (see (4.21)). Hence, $\{\mathbf{q}_j\}_{j=1}^{6}$ has two more degrees of freedom than $\{\mathbf{q}'_j\}_{j=1}^{6}$. Therefore, the parallelogram criterion is more general than Borrelli et al.'s regularity condition.

5. Conclusions

For a surface triangulation obtained from sampling a smooth parametric surface, the approximation accuracy of the Gauss–Bonnet scheme depends very much on how the surface is triangulated. If the domain triangulation is close to a uniform three-directional partition, accurate approximation can be achieved. Otherwise, the approximation error could be very large. We also show that Borrelli et al.'s convergence result for valence $n = 6$ could be derived from our convergence theorems.

Appendix A. Inner products of directional derivatives

The following are all the inner products in (4.10) and (4.11).

$$\langle \mathbf{F}_{\mathbf{d}_j}, \mathbf{F}_{\mathbf{d}_j} \rangle = g_j^2 g_{11} + 2g_j l_j g_{12} + l_j^2 g_{22};$$

$$\langle \mathbf{F}^2_{\mathbf{d}_j}, \mathbf{F}^2_{\mathbf{d}_j} \rangle = g_j^4 g_{1111} + 4g_j^2 l_j^2 g_{1212} + l_j^4 g_{2222} + 4g_j^3 l_j g_{1112} + 2g_j^2 l_j^2 g_{1122} + 4g_j l_j^3 g_{1222};$$

$$\langle \mathbf{F}_{\mathbf{d}_j}, \mathbf{F}^2_{\mathbf{d}_j} \rangle = g_j^3 g_{111} + 2g_j^2 l_j g_{112} + g_j l_j^2 g_{122} + g_j^2 l_j g_{211} + 2g_j l_j^2 g_{212} + l_j^3 g_{222};$$

$$\langle \mathbf{F}_{\mathbf{d}_j}, \mathbf{F}_{\mathbf{d}_{j_+}} \rangle = g_j g_{j_+} g_{11} + g_j l_{j_+} g_{12} + g_{j_+} l_j g_{12} + l_j l_{j_+} g_{22};$$

$$\langle \mathbf{F}_{\mathbf{d}_j}, \mathbf{F}^2_{\mathbf{d}_{j_+}} \rangle = g_j g_{j_+}^2 g_{111} + 2g_j g_{j_+} l_{j_+} g_{112} + g_j l_{j_+}^2 g_{122} + g_{j_+}^2 l_j g_{211} + 2g_{j_+} l_j l_{j_+} g_{212} + l_j l_{j_+}^2 g_{222};$$

$$\langle \mathbf{F}_{\mathbf{d}_{j_+}}, \mathbf{F}^2_{\mathbf{d}_j} \rangle = g_{j_+} g_j^2 g_{111} + 2g_{j_+} g_j l_j g_{112} + g_{j_+} l_j^2 g_{122} + g_j^2 l_{j_+} g_{211} + 2g_j l_{j_+} l_j g_{212} + l_{j_+} l_j^2 g_{222};$$

$$\begin{aligned}\langle \mathbf{F}^2_{\mathbf{d}_j}, \mathbf{F}^2_{\mathbf{d}_{j_+}} \rangle = {} & g_j^2 g_{j_+}^2 g_{1111} + 4g_j g_{j_+} l_j l_{j_+} g_{1212} + l_j^2 l_{j_+}^2 g_{2222} + 2g_j^2 g_{j_+} l_{j_+} g_{1112} \\ & + 2g_{j_+}^2 g_j l_j g_{1112} + g_j^2 l_{j_+}^2 g_{1122} + g_{j_+}^2 l_j^2 g_{1122} + 2g_j l_j l_{j_+}^2 g_{1222} + 2g_{j_+} l_{j_+} l_j^2 g_{1222};\end{aligned}$$

$$\begin{aligned}\langle \mathbf{F}_{\mathbf{d}_j}, \mathbf{F}^3_{\mathbf{d}_j} \rangle = {} & g_j^4 e_{1111} + 3g_j^3 l_j e_{1112} + 3g_j^2 l_j^2 e_{1122} + g_j l_j^3 e_{1222} + g_j^3 l_j e_{2111} + 3g_j^2 l_j^2 e_{2112} \\ & + 3g_j l_j^3 e_{2122} + l_j^4 e_{2222};\end{aligned}$$

$$\begin{aligned}\langle \mathbf{F}_{\mathbf{d}_j}, \mathbf{F}^4_{\mathbf{d}_j} \rangle = {} & g_j^5 e_{11111} + 4g_j^4 l_j e_{11112} + 6g_j^3 l_j^2 e_{11122} + 4g_j^2 l_j^3 e_{11222} + g_j l_j^4 e_{12222} + g_j^4 l_j e_{21111} \\ & + 4g_j^3 l_j^2 e_{21112} + 6g_j^2 l_j^3 e_{21122} + 4g_j l_j^4 e_{21222} + l_j^5 e_{22222};\end{aligned}$$

$$\begin{aligned}\langle \mathbf{F}^2_{\mathbf{d}_j}, \mathbf{F}^3_{\mathbf{d}_j} \rangle = {} & g_j^5 f_{11111} + 3g_j^4 l_j f_{11112} + 3g_j^3 l_j^2 f_{11122} + g_j^2 l_j^3 f_{11222} + 2g_j^4 l_j f_{12111} + 6g_j^3 l_j^2 f_{12112} \\ & + 6g_j^2 l_j^3 f_{12122} + 2g_j l_j^4 f_{12222} + g_j^3 l_j^2 f_{22111} + 3g_j^2 l_j^3 f_{22112} + 3g_j l_j^4 f_{22122} + l_j^5 f_{22222};\end{aligned}$$

$$\begin{aligned}\langle \mathbf{F}_{\mathbf{d}_j}, \mathbf{F}^3_{\mathbf{d}_{j_+}} \rangle = {} & g_j g_{j_+}^3 e_{1111} + 3g_j g_{j_+}^2 l_{j_+} e_{1112} + 3g_j g_{j_+} l_{j_+}^2 e_{1122} + g_j l_{j_+}^3 e_{1222} + g_{j_+}^3 l_j e_{2111} \\ & + 3g_{j_+}^2 l_j l_{j_+} e_{2112} + 3g_{j_+} l_j l_{j_+}^2 e_{2122} + l_{j_+}^3 l_j e_{2222};\end{aligned}$$

$$\begin{aligned}\langle \mathbf{F}_{\mathbf{d}_{j_+}}, \mathbf{F}^3_{\mathbf{d}_j} \rangle = {} & g_{j_+} g_j^3 e_{1111} + 3g_{j_+} g_j^2 l_j e_{1112} + 3g_{j_+} g_j l_j^2 e_{1122} + g_{j_+} l_j^3 e_{1222} + g_j^3 l_{j_+} e_{2111} \\ & + 3g_j^2 l_{j_+} l_j e_{2112} + 3g_j l_{j_+} l_j^2 e_{2122} + l_j^3 l_{j_+} e_{2222};\end{aligned}$$

$$\begin{aligned}\langle \mathbf{F}_{\mathbf{d}_j}, \mathbf{F}^4_{\mathbf{d}_{j_+}} \rangle = {} & g_j g_{j_+}^4 e_{11111} + 4g_j g_{j_+}^3 l_{j_+} e_{11112} + 6g_j g_{j_+}^2 l_{j_+}^2 e_{11122} + 4g_j g_{j_+} l_{j_+}^3 e_{11222} \\ & + g_j l_{j_+}^4 e_{12222} + g_{j_+}^4 l_j e_{21111} + 4g_{j_+}^3 l_j l_{j_+} e_{21112} + 6g_{j_+}^2 l_{j_+}^2 l_j e_{21122} \\ & + 4g_{j_+} l_{j_+}^3 l_j e_{21222} + l_{j_+}^4 l_j e_{22222};\end{aligned}$$

$$\langle \mathbf{F}_{\mathbf{d}_{j_+}}, \mathbf{F}^4_{\mathbf{d}_j} \rangle = g_{j_+} g_j^4 e_{11111} + 4g_{j_+} g_j^3 l_j e_{11112} + 6g_{j_+} g_j^2 l_j^2 e_{11122} + 4g_j g_{j_+} l_j^3 e_{11222} + g_{j_+} l_j^4 e_{12222}$$

$$
\begin{aligned}
&+ g_j^4 l_{j_+} e_{21111} + 4 g_j^3 l_j l_{j_+} e_{21112} + 6 g_j^2 l_j^2 l_{j_+} e_{21122} + 4 g_j l_j^3 l_{j_+} e_{21222} + l_j^4 l_{j_+} e_{22222};\\
\langle \mathbf{F}^2_{\mathbf{d}_j}, \mathbf{F}^3_{\mathbf{d}_{j_+}} \rangle &= g_j^2 g_{j_+}^3 f_{11111} + 3 g_j^2 g_{j_+}^2 l_{j_+} f_{11112} + 3 g_j^2 g_{j_+} l_{j_+}^2 f_{11122} + g_j^2 l_{j_+}^3 f_{11222}\\
&\quad + 2 g_j g_{j_+}^3 l_j f_{12111} + 6 g_j g_{j_+}^2 l_j l_{j_+} f_{12112} + 6 g_j g_{j_+} l_j l_{j_+}^2 f_{12122} + 2 g_j l_j l_{j_+}^3 f_{12222}\\
&\quad + g_{j_+}^3 l_j^2 f_{22111} + 3 g_{j_+}^2 l_j^2 l_{j_+} f_{22112} + 3 g_{j_+} l_j^2 l_{j_+}^2 f_{22122} + l_j^2 l_{j_+}^3 f_{22222};\\
\langle \mathbf{F}^2_{\mathbf{d}_{j_+}}, \mathbf{F}^3_{\mathbf{d}_j} \rangle &= g_{j_+}^2 g_j^3 f_{11111} + 3 g_{j_+}^2 g_j^2 l_j f_{11112} + 3 g_{j_+}^2 g_j l_j^2 f_{11122} + g_{j_+}^2 l_j^3 f_{11222}\\
&\quad + 2 g_{j_+} g_j^3 l_{j_+} f_{12111} + 6 g_{j_+} g_j^2 l_j l_{j_+} f_{12112} + 6 g_j g_{j_+} l_{j_+} l_j^2 f_{12122} + 2 g_{j_+} l_{j_+} l_j^3 f_{12222}\\
&\quad + g_j^3 l_{j_+}^2 f_{22111} + 3 g_j^2 l_{j_+}^2 l_j f_{22112} + 3 g_j l_j^2 l_{j_+}^2 f_{22122} + l_{j_+}^2 l_j^3 f_{22222}.
\end{aligned}
$$

Acknowledgements

The author is grateful to the referees for their carefully reading of the manuscript and for their helpful comments on improving the final version of this paper. The author also wish to thank Ms. Dan Liu for generating Fig. 2.

References

Alboul, L., van Damme, R., 1995. Polyhedral metrics in surface reconstruction: tight triangulation. Technical Report, University of Twente, Department of Applied Mathematics.

Borrelli, V., Cazals, F., Morvan, J.-M., 2003. On the angular defect of triangulations and the point-wise approximation of curvatures. Computer Aided Geometric Design 20 (6), 319–341.

Do Carmo, M.P., 1976. Differential Geometry of Curves and Surfaces. Prentice-Hall, Englewood Cliffs, NJ.

Cazals, F., Pouget, M., 2005. Estimating differential quantities using polynomial fitting of osculating jets. Computer Aided Geometric Design 22 (2), 767–784.

Chen, X., Schmitt, F., 1992. Intrinsic surfaces properties from surface triangulation. In: Sandini, G. (Ed.), Proc. 2nd European Conf. on Computer Vision, Margherita Ligure, Italy, pp. 739–743.

Cohen-Steiner, D., Morvan, J.-M., 2003. Restricted Delaunay triangulations and normal cycle. In: Proc. 19th Annu. ACM Sympos. Comput. Geom.

Douros, I., Buxton, B.F., 2002. Three-dimensional surface curvature estimation using quadric surface patches. Numerisation 3D—Scanning.

Dyn, N., Hormann, K., Kim, S.J., Levin, D., 2001. Optimizing 3d triangulation using discrete curvature analysis. In: Lyche, T., Schmaker, L.L. (Eds.), Mathematical Methods in CAGD. Vanderbilt University Press, pp. 135–146.

Franke, D., 1982. Scattered data interpolation: Tests of some methods. Mathematics of Computation 38 (157), 181–200.

Hamann, B., 1993. Curvature approximation for triangulated surfaces. Computing Suppl. (8), 139–153.

Kim, S.J., Kim, C.H., Levin, D., 2002. Surface simplification using a discrete curvature norm. Computers and Graphics 26 (5), 657–663.

Krsek, P., Pajdla, T., Hlavac, V., 1997. Estimation of differential parameters on triangulated surfaces. In: 21st Workshop of the Austrian Association for Pattern Recognition.

Martin, R., 1998. Estimation of principal curvatures from range data. Internat. J. Shape Modeling 4, 99–111.

Meek, D., Walton, D., 2000. On surface normal and Gaussian curvature approximations given data sampled from a smooth surface. Computer Aided Geometric Design 17, 521–543.

Meyer, M., Desbrun, M., Schröder, P., Barr, A., 2002. Discrete differential geometry operator for triangulated 2-manifolds. In: Proceedings of Visual Mathematics'02, Berlin, Germany.

Peng, J., Li, Q., Kuo, C.J., Zhou, M., 2003. Estimating Gaussian curvature from 3D meshes. SPIE Electronic Image, in press.
Stokely, E., Wu, S.Y., 1992. Surface parameterization and curvature measurement of arbitrary 3d-objects: Five practical methods. IEEE Trans. Pattern Anal. Machine Intelligence 14 (8), 833–840.
Surazhsky, T., Magid, E., Soldea, O., Elber, G., Rivlin, E., 2003. A comparison of Gaussian and mean curvatures estimation methods on triangular meshes. In: 2003 IEEE International Conference on Robotics & Automation (ICRA2003), pp. 1021–1026.
Taubin, G., 1995. Estimating the tensor of curvatures of a surface from a polyhedral approximation. In: Proceedings 5th Intl. Conf. on Computer Vision (ICCV'95), pp. 902–907.
Watanabe, K., Belyaev, A.G., 2001. Meshes: Detection of salient curvature features on polygonal surfaces. Computer Graphics Forum 20 (3).
Wollmann, C., 2000. Estimation of principle curvatures of approximated surfaces. Computer Aided Geometric Design 17, 621–630.
Xu, G., 2004a. Convergence of discrete Laplace–Beltrami operators over surfaces. Comput. Math. Appl. 48, 347–360.
Xu, G., 2004b. Discrete Laplace–Beltrami operators and their convergence. Computer Aided Geometric Design 21, 767–784.
Xu, G., Bajaj, C., 2003. Curvature computations of 2-manifold in $\mathbb{R}^k$. J. Comput. Math. 21 (5), 681–688.